

# A theoretical study on seasonality

Christoph Schmal<sup>1\*</sup>, Jihwan Myung<sup>2</sup>, Hanspeter Herzl<sup>3</sup> and Grigory Bordyugov<sup>1</sup>

<sup>1</sup> Institute for Theoretical Biology, Charité Universitätsmedizin, Berlin, Germany, <sup>2</sup> RIKEN Brain Science Institute, Wako, Japan, <sup>3</sup> Institute for Theoretical Biology, Humboldt Universität zu Berlin, Berlin, Germany

In addition to being endogenous, a circadian system must be able to communicate with the outside world and align its rhythmicity to the environment. As a result of such alignment, external Zeitgebers can entrain the circadian system. Entrainment expresses itself in coinciding periods of the circadian oscillator and the Zeitgeber and a stationary phase difference between them. The range of period mismatches between the circadian system and the Zeitgeber that Zeitgeber can overcome to entrain the oscillator is called an entrainment range. The width of the entrainment range usually increases with increasing Zeitgeber strength, resulting in a wedge-like Arnold tongue. This classical view of entrainment does not account for the effects of photoperiod on entrainment. Zeitgebers with extremely small or large photoperiods are intuitively closer to constant environments than equinoctial Zeitgebers and hence are expected to produce a narrower entrainment range. In this paper, we present theoretical results on entrainment under different photoperiods. We find that in the photoperiod-detuning parameter plane, the entrainment zone is shaped in the form of a skewed onion. The bottom and upper points of the onion are given by the free-running periods in DD and LL, respectively. The widest entrainment range is found near photoperiods of 50%. Within the onion, we calculated the entrainment phase that varies over a range of 12 h. The results of our theoretical study explain the experimentally observed behavior of the entrainment phase in dependence on the photoperiod.

## OPEN ACCESS

### Edited by:

Urs Albrecht,  
University of Fribourg, Switzerland

### Reviewed by:

Sara S. Fonseca Costa,  
University of Fribourg, Switzerland  
Dominen G. M. Beersma,  
University of Groningen, Netherlands

### \*Correspondence:

Christoph Schmal,  
Institute for Theoretical Biology,  
Charité Universitätsmedizin, Philippstr.  
13 Haus 4, Berlin 10115, Germany  
christoph.schmal@charite.de

### Specialty section:

This article was submitted to Sleep and Chronobiology, a section of the journal Frontiers in Neurology

Received: 13 February 2015

Paper pending published:

18 March 2015

Accepted: 16 April 2015

Published: 07 May 2015

### Citation:

Schmal C, Myung J, Herzl H and Bordyugov G (2015) A theoretical study on seasonality. *Front. Neurol.* 6:94.  
doi: 10.3389/fneur.2015.00094

## 1. Introduction

### 1.1. Entrainment

Most living organisms possess an internal clock which enables them to account for the periodically changing environment due to the Earth's rotation. The clock has to be sufficiently precise and, which is sometimes more important, synchronized to the external cues referred to as Zeitgebers. The process of setting the internal clock by Zeitgebers is called entrainment. Light, being one of the strongest Zeitgebers, succumbs to seasonal changes which results in seasonal variations of the light–dark (LD) ratio. The present paper is a systematic investigation of how entrainment of circadian oscillators is influenced by seasonal variations of the Zeitgeber.

### 1.2. Seasonality

The first studies of the circadian seasonality go back nearly 50 years ago, see e.g., Ref. (1). The LD ratio has been identified as one of the factors that influence the phase of circadian entrainment. In agreement with intuition, the LD ratio close to 12 h:12 h was found to be the strongest Zeitgeber (2). In the golden hamster, the phase of entrainment was measured in dependence on the Zeitgeber

period  $T$  for different LD ratios (3), suggesting that phase of entrainment is more sensitive to variations of  $T$  for shorter LD values. Latitude-dependent LD effects in *Drosophila auraria* were reported in Ref. (4), including differences in phase-response curves and the dependence of the entrainment phase on the photoperiod. In fruit flies, it has been found that the morning and evening activity is controlled by two distinctive sets of neurons (5), which support the idea of morning and evening oscillators (6).

More recently, an in-depth study of entrainment of *Neurospora crassa* under different photoperiods resulted in a three-parameter “circadian surface” (7). Using three different strains with free-running periods of  $\tau = 16.5$  h,  $\tau = 22.5$  h, and  $\tau = 29$  h, the phase of entrainment was measured for Zeitgebers of different LD ratios. On the molecular level, differences between responses to varying photoperiods were recently documented (8). The SCN - the central circadian pacemaker in mammals - showed a break up of synchronization under long photoperiods, but synchronization was re-attained after the transition to short days by advancing the decline of the expression of clock genes (8).

Those studies of seasonality were paralleled by computational modeling of circadian systems under Zeitgebers of different amplitudes, periods, LD ratios, and the proportion of the twilight within a day (9). Numerical calculations revealed that the LD ratio shifts the phase of entrainment in a direction which depends on whether the organism is day- or night-active. Another theoretical approach to the studies of phase of entrainment under different photoperiods was to use a simple piece-wise linear PRC model in Ref. (6). The main result was that the activity onset (dusk for night-active and dawn for day-active organisms) can be conserved across a variety of photoperiod conditions. In addition, a large body of the behavior of entrainment phase for different photoperiods and PRC types was produced and thoroughly analyzed (6).

### 1.3. Arnold Tongue

Graphically, entrainment is represented by the Arnold tongue - a triangular region on the “Zeitgeber period - Zeitgeber strength” parameter plane, see Ref. (10–12), compare also Figure 1A. Within the tongue, Zeitgeber enforces its period in the circadian

system. When entrained, the phase of the circadian system assumes a stable relation to the phase of the Zeitgeber in such a way that  $\psi$  - the difference between those two phases - assumes a stable value. The range of period detunings between the Zeitgeber and the circadian system where entrainment occurs is called range of entrainment. Larger Zeitgeber strengths often lead to larger entrainment ranges which results in the characteristic wedge-like shape of the tongue. Within the Arnold tongue, the structure of the isophases has been determined (13), thus making possible to understand how the phase of entrainment changes under variations of Zeitgeber strength and period.

The classical Arnold tongue depicts the entrainment region in dependence on the effective Zeitgeber strength. When considering entrainment by Zeitgebers with different LD ratios, it is often unclear what the effective Zeitgeber strength is under varying LD ratio. Intuitively, one can expect that Zeitgebers with very short or very long light phase should be less potent in entraining the circadian system than a Zeitgeber with a LD ratio close to 12 h:12 h. In this manuscript, we quantify this intuition and compare it to previously published data on entrainment under different seasonal conditions (3, 14, 15).

### 1.4. Arnold Onion

Our main result is the existence of the onion-shaped entrainment zone on the photoperiod-detuning parameter plane, compare Figure 1B. Both tips of the entrainment onion point to free-running periods in complete darkness  $\tau_{DD}$  or constant light  $\tau_{LL}$ . The widest part of the entrainment range is close to the equinoctial photoperiod. The onion entrainment region is skewed to the right or to the left depending on whether  $\tau_{LL}$  is larger or smaller than  $\tau_{DD}$ . Within the entrainment onion, we calculated the phases of entrainment, thus quantifying the claim by Aschoff (1) on the dependence of the entrainment phase on the photoperiod. The skewness of the entrainment onion makes possible achieving all possible phases of entrainment by changing photoperiods. Even for a constant mismatch  $\tau - T$ , i.e., for vertical cross-sections of the Arnold onion, large variations of entrainment phases are found.

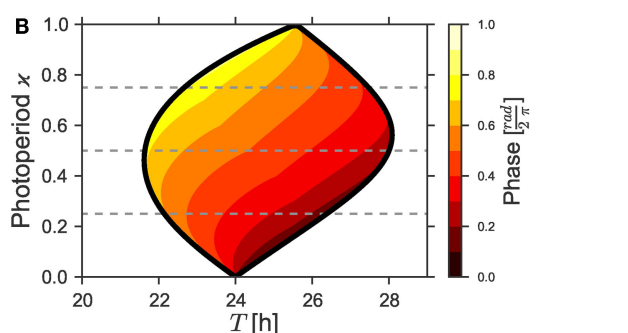
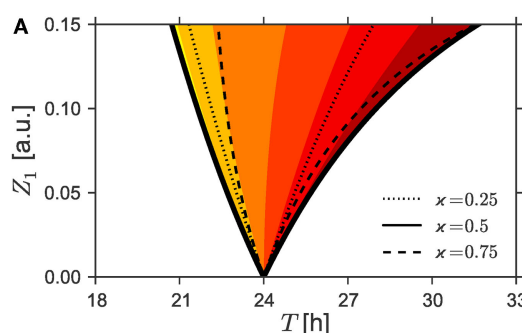


**FIGURE 1 | (A)** 1:1 synchronization region in the  $Z_1 - T$  parameter plane (1:1 Arnold tongue). Dotted, bold, and dashed black lines denote bifurcation curves of periodic solutions as determined by a continuation method for different photoperiods  $x = 0.25$ ,  $x = 0.5$ , and  $x = 0.75$ . Phases of the solutions in the 1:1 synchronization regime to equinox photoperiods (i.e.,  $x = 0.5$ ) are color-coded. **(B)** 1:1 Entrainment range (Arnold onions) and

color-coded phases in the  $x - T$ -plane given a Zeitgeber strength of  $Z_1 = 0.1$ . Dashed lines denote the corresponding photoperiods  $x = 0.25$ ,  $x = 0.5$ , and  $x = 0.75$ . Simulations for both Figures relied on the parameters  $\tau = 24$  h,  $\lambda = 0.5 \text{ h}^{-1}$ , and  $A = 1$ . The color-coded phases in the entrainment regions were determined by a “brute force integration method” as described in Section 2.3.

## 2. Materials and Methods

### 2.1. Mathematical Model

In this paper, we use as an illustrative, conceptual model of the circadian clock, the generic amplitude-phase-oscillator

$$\begin{aligned} \frac{dr(t)}{dt} &= \lambda r(t) (A - r(t)), \\ \frac{d\varphi(t)}{dt} &= 2\pi [\varepsilon \cos^2(\varphi(t)/2) + c(\varepsilon, \tau)], \end{aligned} \quad (1)$$

given in polar coordinates. Here,  $r(t)$  is the radial component while  $\varphi(t)$  describes the phase evolution. The model depends on a small set of generic parameters, namely the oscillator amplitude  $A$ , the amplitude relaxation rate  $\lambda$ , and the intrinsic period  $\tau$ . The parameter  $\varepsilon$  controls the phase velocity  $\frac{d\varphi(t)}{dt}$ : for  $\varepsilon = 0 \text{ h}^{-1}$ , the angular velocity  $\frac{d\varphi(t)}{dt}$  is constant along the whole limit cycle, and for  $\varepsilon \neq 0 \text{ h}^{-1}$ , the limit cycle has sections of faster and slower changing  $\frac{d\varphi(t)}{dt}$  (16).

The internal period  $\tau$  of system (Eq. 1) can be defined by means of the time required for  $\varphi(t)$  to change by  $2\pi$ , i.e.,

$$\tau := 2 \int_0^\pi \frac{d\varphi}{\dot{\varphi}(t)} = \frac{1}{\sqrt{c(c + \varepsilon)}}. \quad (2)$$

It can be noticed that  $\tau$  generally depends on the choice of  $c$  and  $\varepsilon$ . For the sake of tunability, we have chosen the offset  $c(\varepsilon, \tau)$  as

$$c(\varepsilon, \tau) := \sqrt{\tau^{-2} + \varepsilon^2/4} - \varepsilon/2, \quad (3)$$

such that the internal period  $\tau$  in system (Eq. 1) can be freely chosen for any given value of  $\varepsilon$ . If Eq. 1 adopts a uniform phase velocity  $\dot{\varphi}(t) = 2\pi/\tau$  for  $\varepsilon = 0$ , the model is commonly known as the *Poincaré oscillator* (11, 17, 18).

### 2.2. Zeitgeber Input Function

Equation 1 can be transferred into Cartesian coordinates using the definitions  $x(t) := r(t) \cos(\varphi(t))$  and  $y(t) := r(t) \sin(\varphi(t))$ . Including an additive Zeitgeber term, Eq. 1 then reads

$$\begin{aligned} \frac{dx(t)}{dt} &= f_x(x(t), y(t)) + \cos(\alpha) Z(t), \\ \frac{dy(t)}{dt} &= f_y(x(t), y(t)) + \sin(\alpha) Z(t), \end{aligned} \quad (4)$$

where  $Z(t)$  is a scalar  $T$ -periodic Zeitgeber function. An explicit representation of the vector field  $\vec{f}(\vec{x}(t)) := (f_x(x(t), y(t)), f_y(x(t), y(t)))^T$  is given by Eq. 4 in Section S1.1 in Supplementary Material. Finally,  $\alpha$  denotes the “direction” of the perturbation of amount  $Z(t)$  that is applied to the vector field  $\vec{f}(\vec{x}(t))$ . We define this direction by means of the azimuth  $\alpha$  in the polar plane. Using the relations  $\cos(\alpha + \pi) = -\cos(\alpha)$  and  $\sin(\alpha + \pi) = -\sin(\alpha)$ , we can deduce that a phase-shift of  $\pi$  (or  $180^\circ$ ) in the direction  $\alpha$  of the perturbation is tantamount to substituting  $Z(t)$  by  $-Z(t)$ . We will use this relation for the interpretation of **Figure 2A** as well as Figures S2 and S4A in Supplementary Material.

In analogy to common Zeitgeber signals under laboratory conditions, we investigate the entrainment of the *Poincaré Oscillator* to square-wave cycles. Such binary Zeitgeber can be written as

$$Z_{\square}(t) := \begin{cases} Z_1 & \forall t : t \bmod(T) \leq \varkappa T \\ 0 & \text{elsewhere} \end{cases} \quad (5)$$

where we define the photoperiod  $\varkappa := \frac{T_{Z_1}}{T} \in [0, 1]$  as the duration of the phase  $T_{Z_1}$  with an active Zeitgeber signal (i.e.,  $Z(t) = Z_1$ ) divided by the period  $T$  of one Zeitgeber cycle. The photoperiod parameter  $\varkappa$  thus represents the relative duration of the light phase during the day, i.e.,

$$\varkappa = \frac{LL}{LL + DD}.$$

Equation 5 inevitably leads to discontinuities of  $Z_{\square}(t)$  at all time points of changing Zeitgeber intensity. For the sake of the numerical stability of continuation methods applied below, we substitute the piece-wise linear Zeitgeber function (Eq. 5) by a continuous approximation  $Z(t)$ , details are given in Section S1.3 in Supplementary Material.

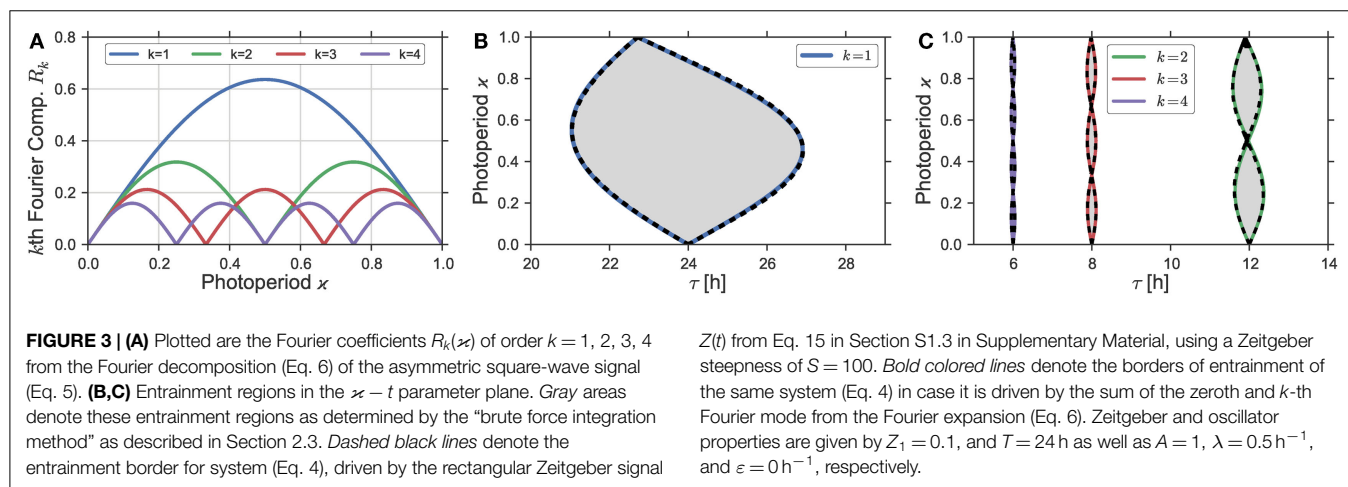
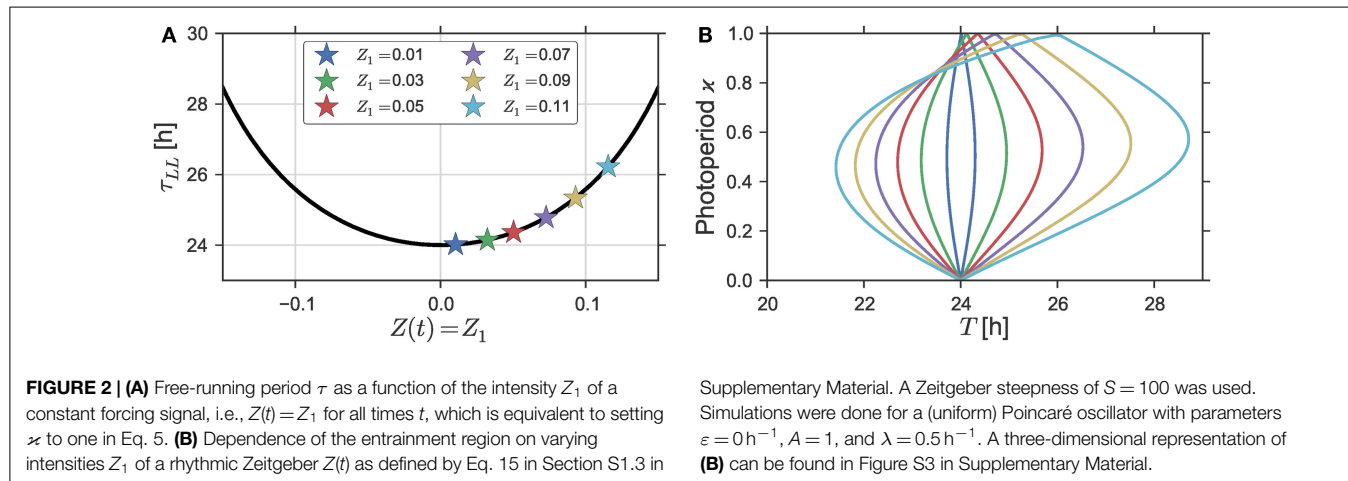
In Section 3.5, we substitute the entrainment signal  $Z(t)$  by the Fourier expansion of the asymmetric square-wave signal  $Z_{\square}(t)$ . The partial sum including the first  $N$  summands of the Fourier series  $\mathcal{F}\{Z(t)\}$  can be written as

$$Z_N(t) = Z_1 \varkappa + \sum_{k=1}^N R_k \cos(2\pi k t / T + \phi), \quad (6)$$

using the abbreviations  $\phi := \arctan(-b_k/a_k)$  and  $R_k := \sqrt{a_k^2 + b_k^2}$  with the Fourier coefficients  $a_k = \frac{Z_1}{k\pi} \sin(2\pi k \varkappa)$  and  $b_k = \frac{Z_1}{k\pi} (1 - \cos(2\pi k \varkappa))$ , see Section S1.4 in Supplementary Material for a derivation of Eq. 6.

### 2.3. Numerics

The color-coded entrainment regions of **Figures 1, 3B,C**, and **5A** as well as the phases in the Figures S4 and S5B in Supplementary Material were calculated by the following “brute force integration method”: firstly, after choosing all Zeitgeber and oscillator parameters, we integrated system (Eq. 4) in Cartesian coordinates for the period of 105 entrainment cycles  $T$  using the *ScientificPYthon* function *odeint*. After that, we determined whether the oscillator is entrained to the Zeitgeber signal by the following procedure: We take the state  $\vec{x}_0$  of the system at the beginning of the 85th entrainment cycle and determine the recurrence times  $t_n$ ,  $n = 0, \dots, N_{\max}$ , to state  $\vec{x}_0$  for all times  $t > 85T$ . We assume that the system has returned to the state  $\vec{x}_0$ , if it has entered a small neighborhood of  $\vec{x}_0$  in state space, defined by an  $\epsilon$ -ball  $B_\epsilon(\vec{x}_0) := \{\vec{x} \in \mathbb{R}^{\dim(\vec{x}_0)} : \|\vec{x} - \vec{x}_0\|_2 < \epsilon\}$  with  $\epsilon = 0.01$  (such that it can return at all, given the inaccuracies of numerical integration). If the recurrence times do not change over time (i.e.,  $|t_{n+1} - t_n| < \delta$  with  $\delta$  being small) and, on top of that, constitute a rational multiple of the Zeitgeber period  $T$ , we consider the oscillator entrained. Finally, we define the phases of  $x(t)$  and  $y(t)$  of the entrained oscillator based on the time a given variable needs to reach a local maximum after the onset of light.



Apart from this “brute force integration method,” we also calculated the borders of entrainment, which are given by bifurcations of the system (Eq. 4). For this purpose, we used two different Continuation software packages: **Figure 2A** as well as Figures S2, S3, S4A, and S5A in Supplementary Material rely on computations done with *XPP-AUTO* (19). All other bifurcation lines in **Figures 1, 2B, 3B,C** as well as **Figure 5A** were computed by means of *AUTO-07p* (20, 21).

### 3. Results

Circadian clocks are endogenous pacemakers, generating oscillations of certain physiological processes with a period of approximately 24 h. One of the central properties of these rhythms is their persistence under constant environmental conditions, i.e., without fluctuating external influences at diel frequency. However, constant environmental conditions are rather the extreme exception in nature. Thus, to pace the rhythmic endogenous processes with the period of the Earth’s rotation is of major importance and was shown to confer a fitness benefit to the organism (22–24). Rhythmic environmental signals that are able to synchronize or entrain the circadian system to their own frequency are called *Zeitgeber* signals (25).

In case of synchronization, the circadian oscillation of a given physiological process and the Zeitgeber signal will establish a stable phase relation  $\psi$ , commonly known as the phase of entrainment (POE). If the system synchronizes at all and in such case the POE will generally be dependent on the intrinsic properties of the circadian system as well as the waveform, intensity, and period of the Zeitgeber signal.

In the next sections, we will systematically investigate the dependency of the entrainment region and the POE on the properties of the oscillator and the Zeitgeber signal by means of modeling approaches. We will show that entrainment under different photoperiod bears many similarities with the classical Arnold tongue picture. The calculated dependence of the POE on the photoperiod parameter  $\varkappa$  and the oscillator’s intrinsic period  $\tau$  will complete our study.

#### 3.1. Mathematical Model

Over the last decades, mathematical models have made a decisive contribution to the understanding of the circadian clockwork among a variety of organisms. While detailed, biochemically motivated models aim to shed light on the interlocking of the circadian clockwork’s cogs and levers in a specific biological context (organisms, cell types, etc.), simple and rather abstract

conceptual oscillator models can be used to understand generic features of the circadian system (26).

Following this tradition of modeling in the field of chrono-biology (9, 27–31), we describe the dynamical properties of the circadian clock by means of a generic amplitude–phase oscillator, see Section 2.1 for details. Given in polar coordinates, the dynamical Eq. 1 define the radial evolution  $r(t)$  in time (i.e., the time-dependent distance from the origin) as well as the phase dynamics  $\varphi(t)$  for a given initial condition  $(r_0, \varphi_0)$ . A small set of only four generic parameters  $\tau$ ,  $A$ ,  $\lambda$ , and  $\varepsilon$  conveniently describes general features of limit cycle oscillators: While  $A$  denotes the amplitude of the oscillator with internal period  $\tau$ , the parameter  $\lambda$  quantifies the rate at which an amplitude perturbation relaxes back to its stable periodic orbit at radius  $r^* = A$ . Parameter  $\varepsilon$  determines the shape of the oscillations. For  $\varepsilon = 0 \text{ h}^{-1}$ , Eq. 1 reduce to a system of uniform phase velocity which is commonly referred to as a *Poincaré oscillator* (17). For  $\varepsilon > 0 \text{ h}^{-1}$ , we introduce a non-uniformity of the phase velocity: on the periodic orbit, there are stretches of a larger and smaller instantaneous phase velocity  $\frac{d\varphi(t)}{dt}$ . We can thus tune the shape of the resulting oscillations (when viewed in Cartesian coordinates) ranging from sinusoidal ( $\varepsilon = 0 \text{ h}^{-1}$ ) to more and more spike-like oscillations ( $\varepsilon > 0 \text{ h}^{-1}$ ), compare also Ref. (16).

### 3.2. Entrainment

Throughout this paper, we consider the effect of a given Zeitgeber by means of a scalar function  $Z(t)$  that forces the system along a certain direction (e.g., the  $x$ - or  $y$ -axis) in the phase-plane, see Eq. 4. Recently, it was demonstrated that oscillators with low amplitudes  $A$  and relaxation rates  $\lambda$  can be more easily entrained by a rhythmic Zeitgeber  $Z(t)$  in comparison to oscillators with large  $A$  and  $\lambda$  (32). Based on this differential responsiveness to a certain Zeitgeber signal, we will term oscillators with a large entrainment region “weak” oscillators while terming oscillators with a narrow entrainment region “strong” oscillators.

As already discussed above, the strength, period, and waveform of a Zeitgeber signal will determine if an oscillator will entrain or not. **Figure 1A** shows the region of 1:1 synchronization in the parameter plane of Zeitgeber intensity  $Z_1$  and period  $T$ . A square-wave Zeitgeber signal with equal periods of light and darkness was assumed to act on a *uniform Poincaré oscillator* with  $\varepsilon = 0 \text{ h}^{-1}$ ,  $A = 1$ ,  $\lambda = 0.5 \text{ h}^{-1}$ , and an intrinsic period of  $\tau = 24 \text{ h}$ . The phases of entrainment, which were normalized to values between 0 and 1, are color-coded. As intuitively expected, narrow entrainment ranges can be observed for a Zeitgeber signal of low strength  $Z_1$ . The entrainment range successively gets broader with an increasing Zeitgeber intensity  $Z_1$ , thus leading to a triangularly shaped structure called Arnold tongue. The tip of this Arnold tongue lies for  $Z_1 = 0$  at a point defined by a vanishing period mismatch (i.e.,  $\tau - T = 0$ ).

Since the effective Zeitgeber strength scales reciprocally with the oscillator amplitude (13), we can interpret the effect of a low or high Zeitgeber intensity  $Z_1$  in analogy to the behavior of a strong or a weak oscillator, respectively. Thus, it follows from **Figure 1A** that strong oscillators with a small range of entrainment exhibit a high sensitivity of their phases of entrainment to the period mismatch  $\tau - T$ . Analogously, weak oscillators with a large

range of entrainment exhibit a low sensitivity of their phase of entrainment.

The discrimination of weak and strong oscillators was used in Ref. (32) to interpret experiments on the tissue level but can even be applied to interpret entrainment data on the organismic level. For example, a comparative study on literature data by Aschoff and Pohl revealed that mammals and birds have a rather narrow entrainment range accompanied by a high sensitivity of the entrainment phase  $\psi$  in comparison to insects, plants, and unicellular organisms (3). These differences could either reflect a differential response to a given Zeitgeber signal or could point to different oscillator properties of the underlying circadian clocks.

An attractive hypothesis to explain such differences in entrainment ranges and phase sensitivities relies on the effect of mutual coupling among clock neurons in the mammalian and avian circadian system. In contrast to unicellular organisms and plants, vertebrates have a highly centralized organization of their circadian master clock, consisting of multiple, densely packed neurons which are thought to mutually couple via neurotransmitters like GABA, VIP, or AVP (33). However, it was shown theoretically that coupling between autonomously oscillating systems can lead to an amplitude expansion as well as an enhancement of the relaxation rates of the oscillators. It can thus reduce the entrainment range of the coupled system in comparison to the behavior of the single oscillators (32, 34). Along these lines, coupling between clock neurons could be the essential difference that explains the narrower entrainment range and higher sensitivity of  $\psi$  with respect to varying period mismatches  $\tau - T$  in mammals and birds. It shall be noted, that the above interpretation for ensembles of cells, which is supported e.g., by entrainment data in Ref. (3, 32), solely holds true where the dynamical behavior of the whole network of coupled oscillators can be approximated by a single-oscillator model. The interpretation of certain other experimental findings might demand the consideration of the underlying network organization: one example is an enhanced sensitivity to Zeitgeber signals during an increasing ensemble amplitude of neuronal activity in a population of clock neurons after short-day entrainment in mice (35). A similar boost of phase-shift capacity after short-day entrainment was found in hamsters (36). These findings, at a first glance counterintuitive in the light of the differences between strong and weak oscillators, could indicate yet to be clarified network mechanisms.

### 3.3. Effects of a Varying Photoperiod

So far, we have discussed the impact of varying Zeitgeber intensity and period mismatch on the entrainment properties of the circadian clock. Organisms living distant from equatorial latitudes are also subject to seasonal changes in the duration of light they receive per day. We now investigate, using our modeling approach, the effect of varying light duration by changing the fraction  $\varkappa$  of one Zeitgeber period  $T$  in which the Zeitgeber signal is active (i.e.,  $Z(t)=Z_1$ ), see Section 2.2 and Section S1.3 in Supplementary Material for technical details. Throughout the rest of this paper, such fraction  $\varkappa$ , which is also termed *duty cycle* in the context of electrical engineering, will be used as synonym for the *photoperiod*. The photoperiod  $\varkappa$  can take values between 0 and 1 and

the extremal values  $\varkappa=0$  and  $\varkappa=1$  are equivalent to constant darkness or constant light conditions, respectively.

**Figure 1B** investigates the region of entrainment in the  $\varkappa-T$  parameter plane for a maximal Zeitgeber intensity of  $Z_1=0.1$ , using the same set of oscillator parameters as in **Figure 1A** (i.e.,  $\varepsilon=0\text{ h}^{-1}$ ,  $A=1$ ,  $\lambda=0.5\text{ h}^{-1}$ , and  $\tau=24\text{ h}$ ). In the first place, one notices that the entrainment region adopts an oval, onion-shaped geometry. Such region that we will term Arnold onion in the following, has its widest range of entrainment near the equinoctial photoperiods at  $\varkappa=0.5$ . It gets narrower for photoperiods differing from equinox and tapers toward extremer photoperiods. The tips of the onion point to entrainment periods  $T$  that are given by the free-running periods of the oscillator under constant darkness ( $\tau_{DD}$ ) or constant light ( $\tau_{LL}$ ), respectively. Thus, the Arnold onion will be tilted (i.e., there is no symmetry along the  $\varkappa$ -axis) in any case where the difference  $\Delta\tau=\tau_{LL}-\tau_{DD}$  does not equal 0.

The Arnold onion represents the main finding of this paper. We continue the manuscript by explaining the following aspects: (i) what determines the tilt of the onion, i.e., whether the onion is skewed toward left or toward right, (ii) what makes the Arnold onion open and close again under change of the photoperiod and how this can be related to the properties of the classical Arnold tongue, and (iii) what is the distribution of the phase of entrainment  $\psi$  within the onion.

### 3.4. Free-Running Periods Determine the Tilt of the Arnold Onion

The influence of a certain Zeitgeber signal can be interpreted as a parametric change in the circadian clocks dynamical system, i.e., a time-dependent change of its set of parameters. Changes in the intensity of a constant environmental signal that can potentially act as a Zeitgeber will thus most probably lead to changes in the oscillation period whenever its parametric effects are not compensated or balanced out. A large body of data has accumulated, showing for a variety of organisms that the free-running period under conditions of a constant light generally depends on the intensity of the illumination (37, 38). Whether such parametric changes lead to an increase or decrease of the free-running period for an increasing light-intensity generally depends on the specificities of the organism under investigation. Aschoff was the first who noticed that day-active animals and green plants typically shorten ( $\tau_{LL}<\tau_{DD}$ ) while night-active animals lengthen ( $\tau_{LL}>\tau_{DD}$ ) their free-running period with an increasing intensity of illumination (37). Only few exceptions have been found to this rule which is now known as *Aschoff's Rule* (39). According to this rule, we expect that the Arnold onions of night-active animals like mice will be tilted to periods larger than their spontaneous frequency  $\tau_{DD}$  under constant darkness. Analogously, Arnold onions of day-active animals and plants are expected to be tilted the other way around.

Since the tips of the Arnold onion are given by the free-running periods  $\tau_{DD}$  (the lower tip) and  $\tau_{LL}$  (upper tip), the tilt of the onion depends on the relation between those free-running periods. **Figure 2A** shows the dependency of the free-running period  $\tau_{LL}$  of a uniform Poincaré Oscillator (i.e.,  $\varepsilon=0\text{ h}^{-1}$ ) to changing intensities of a constant forcing signal  $Z(t)=Z_1$  for all times  $t$ .

The effect of a forcing signal is defined as an additive perturbation along the  $x$ -axis like before [i.e.,  $\alpha=0$  in Eq. 4]. If we take  $Z_1=0$  as the nominal parameter value under constant darkness, a steady increase of the free-running period can be observed for steadily increasing Zeitgeber intensities with  $Z_1>0$ . The only exception is a small range of high Zeitgeber intensities  $Z_1\gg 0$  close before a further increase would lead to arrhythmia (damped oscillations) by driving the system through an *Andronov-Hopf bifurcation*. Therein, we can observe a decline of the free-running period with an increasing Zeitgeber intensity, see **Figure S2** in Supplementary Material. In general, the steepness of such light-intensity-dependent changes of the free-running period is strongly dependent of the oscillator properties. Uniform Poincaré oscillators with higher radial relaxation rates  $\lambda$  or lower amplitudes  $A$  exhibit a steeper increase in  $\tau_{LL}$  upon changing  $Z_1$  compared to oscillators with small values of  $\lambda$  and high values of  $A$ , respectively, compare **Figures S2A,B** in Supplementary Material.

The effects of the maximal Zeitgeber intensity  $Z_1$  on the shape of the Arnold onion are investigated in **Figure 2B**. There, the entrainment regions in the  $\varkappa-T$  parameter plane are plotted for different Zeitgeber intensities  $Z_1$ . As expected from the dependency of the free-running period  $\tau_{LL}$  on the Zeitgeber intensity  $Z_1$ , see **Figure 2A**, we can observe an increasing tilt of the Arnold onion for increasing values of  $Z_1$ . Since the width of the entrainment range of a self-sustained oscillator is usually positively correlated with the amplitude of its entraining Zeitgeber signal (see, e.g., **Figure 1A**), we see, apart from a larger tilt also a broadening of the Arnold onion with increasing Zeitgeber strength.

A peculiarity of the Poincaré Oscillator with  $\varepsilon=0\text{ h}^{-1}$  is the uniform evolution of the oscillators' phase in time. As a direct consequence, the system yields rotation equivariance. Thus, a rotation of the Zeitgeber direction  $\alpha$  by a certain angle  $\beta$  will lead to exactly the same solution apart from a phase-shift of magnitude  $\beta$ , see Section S1.2 in Supplementary Material for further details. This explains the symmetry in **Figure 2A**, namely the fact that both positive and negative constant forcing signals result in increasing  $\tau_{LL}$ . As described in Section 2.2, negative values of  $Z_1$  correspond to a rotation of the Zeitgeber by  $\beta=180^\circ$ , thus leading to phase-shifted solutions with exactly the same period  $\tau_{LL}$  compared to positive signals  $Z(t)$  (corresponding to  $\alpha=0^\circ$ ) of a given intensity  $|Z_1|$ . Regardless of the direction of the forcing signal, we thus obtain an increase in the free-running period  $\tau_{LL}$  with increasing Zeitgeber strength, which mimics the behavior of night-active animals.

In a simple extension of the model, the rotational symmetry of the uniform Poincaré Oscillator can readily be broken by introducing a non-uniform phase evolution as described by Eq. 1 for  $\varepsilon\neq 0\text{ h}^{-1}$ . Such non-uniform oscillator shows a decrease of the free-running period for  $Z_1<0$  and an increase for  $Z_1>0$  if a constant forcing signal is applied, see **Figure S4A** in Supplementary Material. Hence, the corresponding Arnold onions are tilted toward  $\tau_{LL}<\tau_{DD}$  for  $Z_1<0$  and into the opposite direction  $\tau_{LL}>\tau_{DD}$  for  $Z_1>0$ , see **Figure S4B** in Supplementary Material. We are thus able to mimic this general behavior of night-active animals and day-active animals or plants with one generic oscillator model, parameterized by a set of only four generic parameters.

### 3.5. Explaining the Form of the Arnold Onion

It turns out that the onion-like structure of the entrainment zone on the “LD ratio-detuning” parameter plane can be explained with the help of the reduction of the system to its phase dynamics (12). This explanation does not rely on a particular kind of the oscillating system, which we assume to have a most general form of

$$\frac{d\vec{u}}{dt} = \vec{f}(\vec{u}) + \vec{z}(t), \quad (7)$$

where  $\vec{u}(t)$  is a  $N$ -dimensional state variable,  $\frac{d\vec{u}}{dt} = \vec{f}(\vec{u})$  is the autonomous (non-perturbed) equation of the circadian oscillator model and  $\vec{z}(t)$  is an external time-periodic Zeitgeber. It turns out (12, 13) that the dynamics of the phase difference  $\psi$  between the oscillations of  $\vec{u}(t)$  and the Zeitgeber  $\vec{z}(t)$  is determined by the circular convolution integral

$$\frac{d\psi}{dt} = \int_0^T dt \vec{\xi}(t - \psi) \vec{z}(t), \quad (8)$$

where  $\vec{\xi}(t)$  is the infinitesimal phase-response function of the limit cycle in the unperturbed equation  $\frac{d\vec{u}}{dt} = \vec{f}(\vec{u})$ . This convolution integral can be best understood by recalling that a convolution in the time domain is equivalent to the product of the Fourier transforms of the functions  $\vec{\xi}$  and  $\vec{z}$  in the frequency domain.

#### 3.5.1. The Case of Sine-Like PRCs

In the case of Eq. 1 with  $\varepsilon = 0 \text{ h}^{-1}$ , the phase-response function is given by  $\vec{\xi}(t) = (-\sin(\omega t), \cos(\omega t))^T$ , i.e., it has a single Fourier component at the base frequency  $\omega$ . By the convolution theorem, the dynamics of the phase difference will hence be determined only by the first Fourier coefficient of the Zeitgeber  $Z(t)$ . In **Figure 3**, we present the result of the computation of the Arnold onion in a direct way compared to the prediction by the first Fourier mode. **Figure 3A** shows the dependence of the first four Fourier modes of a rectangular Zeitgeber in dependence on the photoperiod  $\varkappa$ , note also Eq. 6. There, we see that the first Fourier mode has its maximum at  $\varkappa = 0.5$  and approaches 0 for  $\varkappa$  close to 0 and 1. Thus, we expect that Zeitgebers with  $\varkappa$  close to 0.5 would have the largest influence on the circadian oscillator and, consequently, would result in a widest range of entrainment. In **Figure 3B**, we plot the Arnold onion calculated with the rectangular Zeitgeber with different photoperiods  $\varkappa$  (bold colored lines) and, for comparison, the Arnold onion calculated using just the sum of zeroth and the first Fourier mode of the same Zeitgeber (dashed black lines). Both lines coincide almost perfectly, which supports our claim that the first Fourier mode of the Zeitgeber determines the entrainment dynamics in Eq. 1 with  $\varepsilon = 0 \text{ h}^{-1}$ .

#### 3.5.2. Higher Order Arnold Onions

So far, we have considered 1:1 entrainment in case of Zeitgeber periods  $T$  that were close to the internal period  $\tau$ . The same logic applies for entrainment by Zeitgebers with periods  $T$  being multiples of the endogenous period  $\tau$  with the only difference that it is the  $k$ -th Fourier mode that matters for entrainment with  $\frac{T}{\tau} \approx k$  for  $k = 1, 2, \dots$ . Depending on the photoperiod

$\varkappa$ , the  $k$ -th Fourier mode of the rectangular Zeitgeber has  $k+1$  zeros, compare **Figure 3A**. The corresponding entrainment zones are consequently organized as  $k$  separate Arnold onions piled on top of each other, see **Figure 3C**. The photoperiods  $\varkappa$  of the zero-width entrainment range are given by the values of  $\varkappa$ , where the corresponding  $k$ -th Fourier mode has a 0. Higher order resonances have also been observed experimentally in the context of circadian entrainment, where the phenomenon is commonly known as *frequency demultiplication* (7, 40, 41).

#### 3.5.3. Beyond Sine-Like PRCs

Even if the PRC of the oscillator contains more than one Fourier mode (as it is the case in Eq. 1 with  $\varepsilon \neq 0 \text{ h}^{-1}$ ), we can still apply the convolution theorem to Eq. 8. For a constant Zeitgeber, be it a 0 as in the case of a DD regime or a positive constant as in the case of a LL regime, all Fourier modes save the zeroth, are equal to 0, thus making no contribution to the dynamics of the phase difference  $\psi$  in Eq. 8. Thus, we expect that even for a general non-sine-like PRC and an arbitrary Zeitgeber with a seasonally driven periodicity, the entrainment zone must close in an onion-like manner at  $\varkappa = 0$  and  $\varkappa = 1$ .

### 3.6. Entrainment Phases Under Varying Photoperiods

Possessing an intrinsic period  $\tau$  that enables the synchronization to environmental Zeitgeber signals allows the circadian clock to pace physiological processes with daily environmental cycles of light and temperature. In the synchronized state, it is actually the phase of entrainment  $\psi$  that schedules diurnal physiological processes within the temporal structure of a solar day. From an evolutionary point of view, parameters that influence the value of  $\psi$  are thus expected to be open to evolutionary adjustment or natural selection. Our current theoretical considerations allow us to study the phase of entrainment  $\psi$  inside the Arnold onions, i.e., for different values of period mismatches and photoperiods.

We have shown in Section 3.2 that the entrainment range of a given self-sustained oscillator which is subject to a periodic Zeitgeber signal broadens with an increasing Zeitgeber strength  $Z_1$ . Interestingly, it is found that, regardless of the Zeitgeber strength, the phase of entrainment  $\psi$  can vary only within a range of approximately  $180^\circ$  across the entrainment interval of a classical Arnold tongue (13). Consequently, the sensitivity of the phase  $\psi$  to changes in the period mismatch  $\tau - T$  gets smaller with increasing Zeitgeber intensities, see **Figure 1A**. Since we have proven in the last section that a rectangular Zeitgeber has its largest impact at equinoctial photoperiods ( $\varkappa = 0.5$ ), we expect the phase-sensitivity on the inside of a given Arnold onion to be smallest at  $\varkappa = 0.5$  while it should get larger the further we get away from equinox. This theoretical expectation is confirmed numerically by **Figure 4**, where we have plotted the phase of entrainment versus the period mismatch for equinoctial ( $\varkappa = 0.5$ ) as well as extremely short ( $\varkappa = 0.05$ ) and long ( $\varkappa = 0.95$ ) photoperiods. Interestingly, such behavior can also be found in experimental studies using golden hamsters (*Mesocricetus auratus*) (3). When forced by light-dark cycles of different periods  $T$ , these animals show a relatively wide range of entrainment and a low phase-sensitivity for equinoctial photoperiods  $\varkappa = 0.5$ . In contrast, a

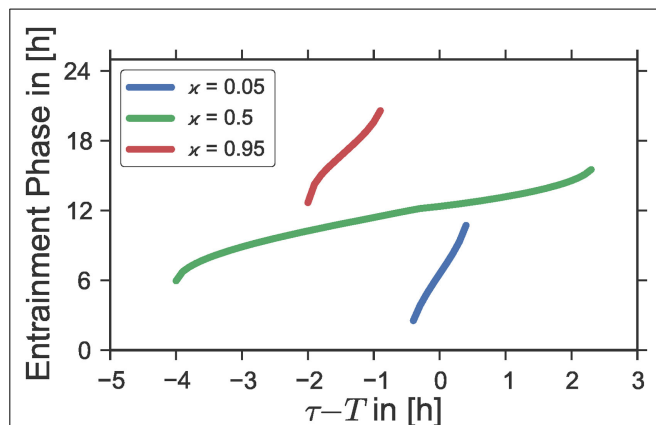


**FIGURE 4 |** Entrainment phases  $\psi$  as a function of the period mismatch  $\tau - T$  between the intrinsic oscillator period  $\tau$  and the Zeitgeber period  $T$  for different photoperiods  $\varkappa$ . The curves correspond to horizontal cross-section of Figure 1B at the ordinate positions  $\varkappa = 0.05$ ,  $\varkappa = 0.5$ , and  $\varkappa = 0.95$ , respectively; i.e., the same Zeitgeber intensity  $Z_1$  and oscillator properties  $\varepsilon$ ,  $A$ ,  $\lambda$ , and  $\tau$  were used as those underlying the simulations in Figure 1B.

high phase-sensitivity accompanied by a narrow range of entrainment could be observed for extremely short photoperiods where a 1 h light-pulse per Zeitgeber period  $T$  was applied.

**Figure 5A** shows the Arnold onions in the photoperiod ( $\varkappa$ ) – internal period ( $\tau$ ) parameter plane for two different maximal Zeitgeber intensities, namely  $Z_1 = 0.05$  and  $Z_1 = 0.1$ . Please note that a right-tilted Arnold onion in the  $\varkappa - T$  parameter plane appears as a left-tilted onion in the  $\varkappa - \tau$  parameter plane and *vice versa*. Hence, **Figure 5A** shows an oscillator with  $\tau_{LL} > \tau_{DD}$  and owing to Aschoff's rule is representative for night-active animals. Again, the amount of tilt and the entrainment region is determined by the maximal Zeitgeber intensity  $Z_1$  - the larger tilt and entrainment region is generated by a larger  $Z_1$ .

In **Figure 5B**, we show the entrainment phase  $\psi$  in dependence on the photoperiod  $\varkappa$  for three sections through the Arnold onion for  $Z_1 = 0.1$ , which are denoted as vertical dashed lines in **Figure 5A**. The difference between the sections is the choice of the internal period  $\tau$ . The variation in the internal periods can be interpreted as different period phenotypes of the same organism, either describing natural variation or specific clock mutants. In the first case with  $\tau = 22$  h, the vertical line crosses just one side of the onion and the entrainment phase does not span a 12 h range as discussed in Ref. (13). In the second case with  $\tau = 26$  h, the situation is mirrored: the line crosses the right border of the onion and the entrainment phase varies again within a range smaller than 12 h. With  $\tau = 23.5$  h, however, both borders of the onion can be reached by varying  $\varkappa$  and the entrainment phase spans a broader range of values, appearing above as well as below the L to D transition in **Figure 5**. In this case, under variation of the photoperiod  $\varkappa$ , the phase of entrainment spans a range considerably larger than 12 h. We additionally note that since it is the difference between the periods  $\tau - T$  that determines the form of the Arnold onion, similar results can be obtained with a constant  $\tau$ , but rather different Zeitgeber periods  $T$ .

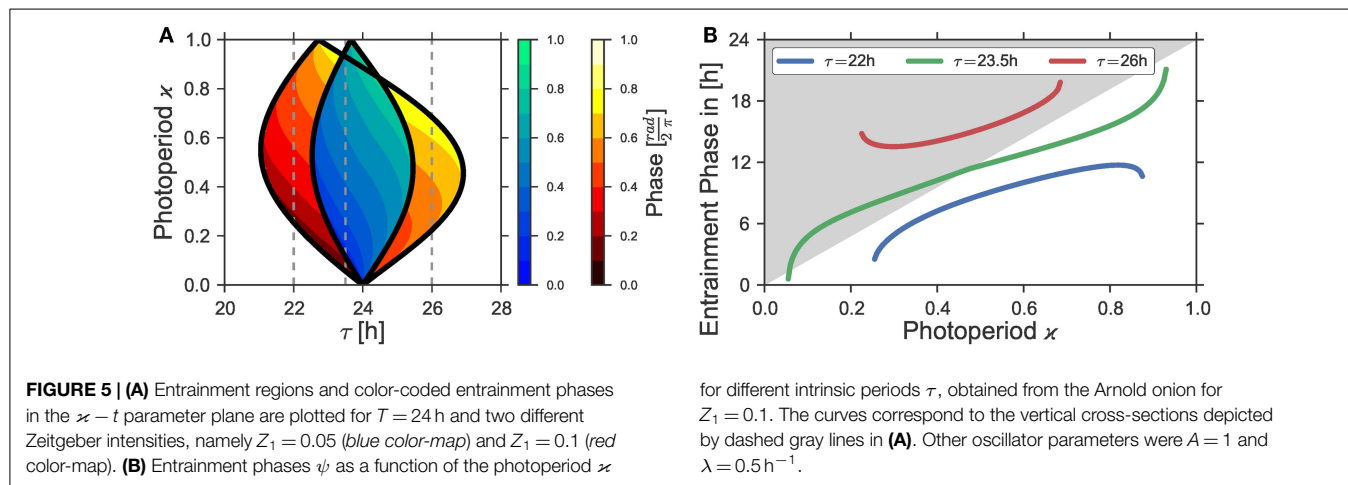
## 4. Discussion

Our main finding in this manuscript is the concept of the Arnold onion, which formalizes the notion of entrainment of circadian systems under different photoperiods. Using a generic model of the circadian clock we provided theoretical evidence that the entrainment region in the photoperiod ( $\varkappa$ ) – Zeitgeber period ( $T$ ) parameter plane constitutes an onion-shaped geometry, see **Figure 1B**. This Arnold onion has its widest entrainment range close to equinox and tapers for extreme photoperiods toward the free-running periods  $\tau_{LL}$  and  $\tau_{DD}$  under constant conditions. From this it follows that the Arnold onion is tilted, whenever the free-running period under a constantly *active* forcing signal ( $\tau_{LL}$ ) is considerably different compared to its period under a constantly *inactive* forcing signal ( $\tau_{DD}$ ), i.e.,  $\Delta\tau = \tau_{LL} - \tau_{DD} \neq 0$ , see e.g., **Figure 2**. Owing to Aschoff's rule, we thus expect a left-tilted Arnold onion in case of diurnal animals or plants while expecting a right-tilted Arnold onion for nocturnal animals. This proposed behavior is confirmed by a numerical study of the Arnold onions from a previously published molecular model of the plant model organism *Arabidopsis thaliana*, see Figure S5 in Supplementary Material.

A direct implication of the tilt of the Arnold onion is that the entrainment range along the photoperiodic axis is not symmetrical around equinoctial photoperiods ( $\varkappa = 0.5$ ). If the entraining period  $T$  is closer to  $\tau_{DD}$  than to  $\tau_{LL}$ , then the oscillator will better entrain to extremely short photoperiods than to extremely long photoperiods and *vice versa* if  $T$  is closer to  $\tau_{LL}$ . This theoretical prediction is consistent with experimental findings in a set of organisms (14, 15). For example, it was found that the drinking behavior of squirrel monkeys (*Saimiri sciureus*) remained synchronized with the 24 h rhythms of light pulses even for extremely short photoperiods while the new world monkeys were not able to entrain to photoperiods longer than 21 h (i.e., LD21:3 or  $\varkappa = 0.875$ ) (15).

Apart from light, temperature cycles can act as Zeitgeber signals among a variety of organisms and tissues (42, 43). One of the most striking features of circadian clocks is temperature compensation, i.e., the relative independence of the circadian clocks' free-running rhythm under constant ambient temperatures of different magnitude, at least inside the physiologically relevant range (44, 45). Since a mismatch between  $\tau_{LL}$  and  $\tau_{DD}$  is a necessary prerequisite for observing a tilt of the Arnold onion, such behavior is *not* expected to occur in temperature compensated circadian clocks with temperature pulses being used as an entrainment cue.

Finally, we investigated systematically how oscillator and Zeitgeber properties determine the phase of entrainment: Our results suggest an increasing phase-sensitivity on the period mismatch  $\tau - T$  with an increasing distance from equinoctial photoperiods. It is thus expected that variations in the driving period  $T$  lead to larger changes of the phase of entrainment under long or short photoperiods when compared to equinox. This has been observed for experimental studies, e.g., in golden hamsters (*Mesocricetus auratus*) or fruit flies (*Drosophila pseudoobscura*) (3). Analogously, we can deduce that for a fixed Zeitgeber period  $T$ , small variations of the internal period  $\tau$  will have an increasing impact on the resulting entrainment phase under photoperiods



that increasingly differ from equinox. On the organismal level, the phase of entrainment can be associated with the chronotype of an organism (13). Thus, the distribution of different chronotypes in a population of a given species is expected to be broader under extreme photoperiods compared to equinoctial ones. On the tissue level, small variations of the intrinsic oscillator properties, e.g., of single neurons, could lead to more dramatic phase variations under extreme photoperiods when compared to equinox. Given the experimentally observed differences of the internal period across different sections in the SCN (46, 47), the higher phase-sensitivity found by our modeling approach could contribute to explain the drastic phase heterogeneity of up to  $180^\circ$  under extremely long photoperiods (48).

From an evolutionary point of view, the entrainment of the circadian clock by rhythmic Zeitgeber signals is of major importance. It allows an organism to phase-lock or schedule (circadian clock regulated) physiological processes around the day. Daily changes of environmental cues can thus be anticipated and optimally used. Furthermore, it opens the possibility to use the time of the day as an ecological niche (49). However, apart from adaption to daily environmental changes, organisms also adapted to seasonal changes of environmental properties. A plethora of physiological processes among a variety of organisms have been reported to react on changes in day-length, a phenomenon commonly known as *photoperiodism*: it has been shown that the photoperiod affects the growth and development of plants and triggers their onset of flowering (50, 51), triggers the induction of diapause in insects (52), and has an impact on the reproduction and the onset of hibernation in mammals (53–55). *Erwin Bünning* pioneered the proposition that it is also the circadian clock that tracks seasons by sensing the photoperiod (56). A flexible phase of entrainment might confer an advantage with respect to the adaption or evolutionary adjustment to seasonally changing demands on an organism. From the viewpoint of the flexibility of the entrainment phase, the Arnold onion offers a richer phase dynamics in comparison to the classical Arnold tongue. In the latter, the 12 h range of entrainment phase is achieved only by variations along the horizontal axis, i.e., by changing either the internal period  $\tau$  or the Zeitgeber period  $T$ , see Ref. (16). In the case of the Arnold onion, variations both in periods  $\tau$  and  $T$  as well as variations in

the photoperiod  $\alpha$  can lead to variability of the entrainment phase even beyond the range of 12 h.

Throughout our studies, we investigated the effect of varying photoperiods among Zeitgeber signals that switch in a binary fashion between states of high ( $Z(t) = Z_1$ ) and low intensities ( $Z(t) = 0$ ). This can only be reached under laboratory conditions. Organisms living under natural environmental conditions are usually faced with complex twilight transitions, photoperiods, and variances of light-intensity and quality due to weather. All these properties vary in a latitude- and altitude-dependent fashion while seasons pass (57). Additionally, gating phenomena on the molecular or behavioral level can influence the effective Zeitgeber strength a given organism can process. It has been shown, for example, that the light input pathway in plants is regulated by the circadian clock itself (58, 59) while sleeping behavior or burrowing can limit the amount of light received by mammals (60).

A certain amount of care should be taken with the interpretation of the dynamics on large networks of coupled oscillators: our current analysis applies to a cluster of synchronizing cells where the group behavior can be approximated by the average, i.e., when the coupling is strong, the network connections are isotropic and the population is homogeneous. Any deviation from the average behavior would imply a particular structural quality of the network. Electrophysiological (35, 61) as well as reporter gene (46, 48) data suggest a redistribution of network properties and organization under varying photoperiods in the suprachiasmatic nuclei of mice. This in turn is likely to affect the sensitivity of the whole network to Zeitgeber signals, thus potentially altering the effective Zeitgeber intensity. However, our current work does help set a theoretical baseline so we can pick up the unique bias in a given network. Furthermore, it still yields an attractive explanation for organismal data as given, e.g., in Ref. (3, 14, 15).

Finally, it should be noted that although light appears to be the most important Zeitgeber in most animals and “higher” plants, a variety of other signals like temperature cycles (42, 59) or odor (62) can additionally act as an entrainment cue. Since the importance of the individual Zeitgeber signals relative to each other is not known yet, an integrative view on the entrainment given all these entrainment cues at parallel remains challenging. If any of the above mentioned phenomena impacts the

effective Zeitgeber strength in a photoperiod dependent manner, the resulting onion-shaped geometry might differ from its rather symmetric shape as depicted in **Figure 1B** (e.g., broader ranges of entrainment under short-day compared to long-day conditions or *vice versa*). However, an analysis of these complex yet interesting variations in the effective Zeitgeber signal a given organism can sense will be subject of future investigations.

## Author Contributions

CS performed numerical computations and wrote text, JM designed the study, GB wrote text and designed the study, HH conceived the study.

## References

- Aschoff J. Phasenlage der Tagesperiodik in Abhängigkeit von Jahreszeit und Breitengrad. *Oecologia* (1969) **3**(2):125–65. doi:10.1007/BF00416979
- Aschoff J, Daan S, Figala J, Müller K. Precision of entrained circadian activity rhythms under natural photoperiodic conditions. *Naturwissenschaften* (1972) **59**(6):276–7. doi:10.1007/BF00610214
- Aschoff J, Pohl H. Phase relations between a circadian rhythm and its Zeitgeber within the range of entrainment. *Naturwissenschaften* (1978) **65**(2):80–4. doi:10.1007/BF00440545
- Pittendrigh CS, Takamura T. Latitudinal clines in the properties of a circadian pacemaker. *J Biol Rhythms* (1989) **4**(2):105–23. doi:10.1177/074873048900400209
- Stoleru D, Peng Y, Agosto J, Rosbash M. Coupled oscillators control morning and evening locomotor behaviour of *Drosophila*. *Nature* (2004) **431**(7010):862–8. doi:10.1038/nature02926
- Pittendrigh CS, Daan S. A functional analysis of circadian pacemakers in nocturnal rodents. *J Comp Physiol* (1976) **106**(3):291. doi:10.1007/BF01417859
- Rémi J, Merrow M, Roenneberg T. A circadian surface of entrainment: varying T,  $\tau$ , and photoperiod in *Neurospora crassa*. *J Biol Rhythms* (2010) **25**(5):318–28. doi:10.1177/0748730410379081
- Sosniyenko S, Parkanová D, Illnerová H, Sládek M, Sumová A. Different mechanisms of adjustment to a change of the photoperiod in the suprachiasmatic and liver circadian clocks. *Am J Physiol Regul Integr Comp Physiol* (2010) **298**(4):R959–71. doi:10.1152/ajpregu.00561.2009
- Wever R. Zum Mechanismus der biologischen 24-Stunden-Periodik. *Kybernetik* (1964) **2**(3):127–44. doi:10.1007/BF00306797
- Arnold V. *Geometrical Methods in the Theory of Ordinary Differential Equations*. 2nd ed. New York, NY: Springer (1988).
- Glass L, Bélair J. Continuation of Arnold tongues in mathematical models of periodically forced biological oscillators. In: Othmer HG, editor. *Nonlinear Oscillations in Biology and Chemistry*. New York: Springer Verlag Berlin Heidelberg (1986). p. 232–43.
- Pikovsky A, Rosenblum M, Kurths J, Hilborn RC. *Synchronization: A Universal Concept in Nonlinear Sciences*. (Vol. 2). Cambridge, IN: Cambridge University Press (2002).
- Granada AE, Bordyugov G, Kramer A, Herzl H. Human chronotypes from a theoretical perspective. *PLoS One* (2013) **8**(3):e59464. doi:10.1371/journal.pone.0059464
- DeCoursey PJ. LD ratios and the entrainment of circadian activity in a nocturnal and a diurnal rodent. *J Comp Physiol* (1972) **78**(3):221–35. doi:10.1007/BF00697656
- Sulzman FM, Fuller CA, Moore-Ede MC. Circadian entrainment of the squirrel monkey by extreme photoperiods: interactions between the phasic and tonic effects of light. *Physiol Behav* (1982) **29**(4):637–41. doi:10.1016/0031-9384(82)90232-3
- Granada AE, Herzl H. How to achieve fast entrainment? the timescale to synchronization. *PLoS One* (2009) **4**(9):e7057. doi:10.1371/journal.pone.0007057
- Glass L, Mackey MC. *From Clocks to Chaos: The Rhythms of Life*. Princeton, NJ: Princeton University Press (1988).
- Glass L, Sun J. Periodic forcing of a limit-cycle oscillator: fixed points, Arnold tongues, and the global organization of bifurcations. *Phys Rev E Stat Phys Plasmas Fluids Relat Interdiscip Topics* (1994) **50**(6):5077. doi:10.1103/PhysRevE.50.5077
- Ermentrout B. *Simulating, Analyzing, and Animating Dynamical Systems: A Guide to XPPAUT for Researchers and Students*. Philadelphia, PA: SIAM (2002).
- Doedel EJ. AUTO, a program for the automatic bifurcation analysis of autonomous systems. *Cong Numer* (1981) **30**:265–384.
- Doedel EJ, Champneys AR, Fairgrieve TF, Kuznetsov YA, Sandstede B, Wang X. *AUTO97: Continuation and Bifurcation Software for Ordinary Differential Equations (with HomCont)*. Technical Report. Montreal: Concordia University (1997).
- Dodd AN, Salathia N, Hall A, Kevei E, Toth R, Nagy F, et al. Plant circadian clocks increase photosynthesis, growth, survival, and competitive advantage. *Science* (2005) **309**(5734):630–3. doi:10.1126/science.1115581
- Michael TP, Salomé PA, Hannah JY, Spencer TR, Sharp EL, McPeek MA, et al. Enhanced fitness conferred by naturally occurring variation in the circadian clock. *Science* (2003) **302**(5647):1049–53. doi:10.1126/science.1082971
- Ouyang Y, Andersson CR, Kondo T, Golden SS, Johnson CH. Resonating circadian clocks enhance fitness in cyanobacteria. *Proc Natl Acad Sci U S A* (1998) **95**(15):8660–4. doi:10.1073/pnas.95.15.8660
- Aschoff J. Zeitgeber der tierischen Tagesperiodik. *Naturwissenschaften* (1954) **41**(3):49–56. doi:10.1007/BF00634164
- Roenneberg T, Chua EJ, Bernardo R, Mendoza E. Modelling biological rhythms. *Curr Biol* (2008) **18**(17):R826–35. doi:10.1016/j.cub.2008.07.017
- Kalmus H, Wigglesworth L. Shock excited systems as models for biological rhythms. *Cold Spring Harbor Symposia on Quantitative Biology*. (Vol. 25). Cold Spring Harbor, LI: Cold Spring Harbor Laboratory Press (1960). p. 211–6.
- Klatter K. General properties of oscillating systems. *Cold Spring Harbor Symposia on Quantitative Biology*. (Vol. 25), Cold Spring Harbor, LI: Cold Spring Harbor Laboratory Press (1960). p. 185–7.
- Pavlidis T. *Biological Oscillators: Their Mathematical Analysis*. New York: Academic Press, Inc. (1973).
- Pittendrigh C, Bruce V, Kaus P. On the significance of transients in daily rhythms. *Proc Natl Acad Sci U S A* (1958) **44**(9):965–73. doi:10.1073/pnas.44.9.965
- Winfree AT. Integrated view of resetting a circadian clock. *J Theor Biol* (1970) **28**(3):327–74. doi:10.1016/0022-5193(70)90075-5
- Abraham U, Granada AE, Westermark PO, Heine M, Kramer A, Herzl H. Coupling governs entrainment range of circadian clocks. *Mol Syst Biol* (2010) **6**:438. doi:10.1038/msb.2010.92
- Aton SJ, Herzog ED. Come together, right now: synchronization of rhythms in a mammalian circadian clock. *Neuron* (2005) **48**(4):531–4. doi:10.1016/j.neuron.2005.11.001
- Bordyugov G, Granada AE, Herzl H. How coupling determines the entrainment of circadian clocks. *Eur Phys J B* (2011) **82**:227–34. doi:10.1140/epjb/e2011-20337-1
- vanderLeest HT, Rohling JHT, Michel S, Meijer JH. Phase shifting capacity of the circadian pacemaker determined by the SCN neuronal network organization. *PLoS One* (2009) **4**(3):e4976. doi:10.1371/journal.pone.0004976
- Evans JA, Elliott JA, Gorman MR. Photoperiod differentially modulates photic and nonphotic phase response curves of hamsters. *Am J Physiol Regul Integr Comp Physiol* (2004) **286**(3):R539–46. doi:10.1152/ajpregu.00456.2003

## Acknowledgments

We would like to thank Matthew Kondoff for critical comments on the manuscript. **Funding:** We acknowledge the financial support from the DFG through the grant BO 3612/2-1 and the RIKEN Incentive Research Project (G1E-54500).

## Supplementary Material

The Supplementary Material for this article can be found online at <http://journal.frontiersin.org/article/10.3389/fneur.2015.00094/abstract>

37. Aschoff J. Exogenous and endogenous components in circadian rhythms. *Cold Spring Harb Symp Quant Biol* (1960) **25**:11–28. doi:10.1101/SQB.1960.025.01.004
38. Aschoff J. Comparative physiology: diurnal rhythms. *Annu Rev Physiol* (1963) **25**(1):581–600. doi:10.1146/annurev.ph.25.030163.003053
39. Pittendrigh CS. Circadian rhythms and the circadian organization of living systems. *Cold Spring Harb Symp Quant Biol* (1960) **25**:159–84. doi:10.1101/SQB.1960.025.01.015
40. Bruce VG. Environmental entrainment of circadian rhythms. *Cold Spring Harb Symp Quant Biol* (1960) **25**:29–48. doi:10.1101/SQB.1960.025.01.005
41. Erzberger A, Hampf G, Granada AE, Albrecht U, Herzl H. Genetic redundancy strengthens the circadian clock leading to a narrow entrainment range. *J R Soc Interface* (2013) **10**(84):20130221. doi:10.1098/rsif.2013.0221
42. Buhr ED, Yoo S-H, Takahashi JS. Temperature as a universal resetting cue for mammalian circadian oscillators. *Science* (2010) **330**(6002):379–85. doi:10.1126/science.1195262
43. McClung CR, Davis SJ. Ambient thermometers in plants: from physiological outputs towards mechanisms of thermal sensing. *Curr Biol* (2010) **20**(24):R1086–92. doi:10.1016/j.cub.2010.10.035
44. Mayer W. Besonderheiten der circadianen Rhythmis bei Pflanzen verschiedener geographischer Breiten. *Planta* (1966) **70**(3):237–56. doi:10.1007/BF00396490
45. Zimmerman WF, Pittendrigh CS, Pavlidis T. Temperature compensation of the circadian oscillation in *Drosophila pseudoobscura* and its entrainment by temperature cycles. *J Insect Physiol* (1968) **14**(5):669–84. doi:10.1016/0022-1910(68)90226-6
46. Myung J, Hong S, Hatanaka F, Nakajima Y, De Schutter E, Takumi T. Period coding of Bmal1 oscillators in the suprachiasmatic nucleus. *J Neurosci* (2012) **32**(26):8900–18. doi:10.1523/JNEUROSCI.5586-11.2012
47. Noguchi T, Watanabe K, Ogura A, Yamaoka S. The clock in the dorsal suprachiasmatic nucleus runs faster than that in the ventral. *Eur J Neurosci* (2004) **20**(11):3199–202. doi:10.1111/j.1460-9568.2004.03784.x
48. Evans J, Leise T, Castanon-Cervantes O, Davidson A. Dynamic interactions mediated by nonredundant signaling mechanisms couple circadian clock neurons. *Neuron* (2013) **80**(4):973–83. doi:10.1016/j.neuron.2013.08.022
49. Hut RA, Kronfeld-Schor N, van der Vinne V, De la Iglesia H. In search of a temporal niche: environmental factors. *Prog Brain Res* (2012) **199**:281–304. doi:10.1016/B978-0-444-59427-3.00017-4
50. Garner WW, Allard HA. Effect of the relative length of day and night and other factors of the environment on growth and reproduction in plants. *Mon Weather Rev* (1920) **48**(7):415–415. doi:10.1175/1520-0493(1920)48<415b:EOTRLO>2.0.CO;2
51. Johansson M, Staiger D. Time to flower: interplay between photoperiod and the circadian clock. *J Exp Bot* (2015) **66**(3):719–30. doi:10.1093/jxb/eru441
52. Masaki S. Seasonal adaptations of insects as revealed by latitudinal diapause clines. *Entomol Sci* (1999) **2**(4):539–49.
53. Coomans CP, Ramkisoensing A, Meijer JH. The suprachiasmatic nuclei as a seasonal clock. *Front Neuroendocrinol* (2015) **37**:29–42. doi:10.1016/j.yfrne.2014.11.002
54. Ruby NF, Dark J, Heller HC, Zucker I. Ablation of suprachiasmatic nucleus alters timing of hibernation in ground squirrels. *Proc Natl Acad Sci U S A* (1996) **93**(18):9864–8. doi:10.1073/pnas.93.18.9864
55. Shinomiya A, Shimmura T, Nishiwaki-Ohkawa T, Yoshimura T. Regulation of seasonal reproduction by hypothalamic activation of thyroid hormone. *Front Endocrinol (Lausanne)* (2014) **5**:12. doi:10.3389/fendo.2014.00012
56. Bünning E. Die endonome Tagesrhythmis als Grundlage der photoperiodischen Reaktion. *Ber Dtsch Bot Ges* (1936) **54**(10):590–607.
57. Hut RA, Paolucci S, Dor R, Kyriacou CP, Daan S. Latitudinal clines: an evolutionary view on biological rhythms. *Proc Biol Sci* (2013) **280**(1765):20130433. doi:10.1098/rspb.2013.0433
58. Fankhauser C, Staiger D. Photoreceptors in *Arabidopsis thaliana*: light perception, signal transduction and entrainment of the endogenous clock. *Planta* (2002) **216**(1):1–16. doi:10.1007/s00425-002-0831-4
59. Millar AJ. Input signals to the plant circadian clock. *J Exp Bot* (2004) **55**(395):277–83. doi:10.1093/jxb/erh034
60. Hut RA, Oort BE, Daan S. Natural entrainment without dawn and dusk: the case of the European ground squirrel (*Spermophilus citellus*). *J Biol Rhythms* (1999) **14**(4):290–9. doi:10.1177/074873099129000812
61. vanderLeest HT, Houben T, Michel S, Deboer T, Albus H, Vansteensel MJ, et al. Seasonal encoding by the circadian pacemaker of the SCN. *Curr Biol* (2007) **17**(5):468–73. doi:10.1016/j.cub.2007.01.048
62. Abraham U, Saleh M, Kramer A. Odor is a time cue for circadian behavior. *J Biol Rhythms* (2013) **28**(1):26–37. doi:10.1177/0748730412469353

**Conflict of Interest Statement:** The authors declare that the research was conducted in the absence of any commercial or financial relationships that could be construed as a potential conflict of interest.

Copyright © 2015 Schmal, Myung, Herzl and Bordugov. This is an open-access article distributed under the terms of the Creative Commons Attribution License (CC BY). The use, distribution or reproduction in other forums is permitted, provided the original author(s) or licensor are credited and that the original publication in this journal is cited, in accordance with accepted academic practice. No use, distribution or reproduction is permitted which does not comply with these terms.